atmosphere

MDPI

Article

Impact of Precipitation with Different Intensity on $PM_{2.5}$ over Typical Regions of China

Xin Zhao [1,2], Yue Sun [1], Chuanfeng Zhao [1,*] and Huifei Jiang [2]

1 State Key Laboratory of Earth Surface Processes and Resource Ecology, College of Global Change and Earth System Science, Beijing Normal University, Beijing 100875, China; 18801057273@163.com (X.Z.); sunyue@mail.bnu.edu.cn (Y.S.)

2 College of Resource and Environment, China Agricultural University, Beijing 100193, China; huifeijiang@gmail.com

* Correspondence: czhao@bnu.edu.cn; Tel.: +86-010-5880-2171

Received: 25 July 2020; Accepted: 22 August 2020; Published: 26 August 2020

Abstract: Atmospheric aerosol pollution has significant impacts on human health and economic society. One of the most efficient way to remove the pollutants from the atmosphere is wet deposition. This study selected three typical atmospheric pollution regions in China, the Beijing-Tianjin-Hebei (BTH), the Yangtze River Delta (YRD) and the Pearl River Delta (PRD) regions, as research areas, and used the hourly precipitation and $PM_{2.5}$ mass concentration data from 2015 to 2017 to investigate the removal impacts of precipitation on $PM_{2.5}$. The $PM_{2.5}$ mass concentration difference before and after the hourly precipitation events was used to denote as the impacts of precipitation. Hourly precipitation event was selected so that the time difference between two $PM_{2.5}$ observations was short enough to limit the $PM_{2.5}$ change caused by other factors. This study focused on the differences in the removal effect of precipitation on $PM_{2.5}$ under different precipitation intensities and pollution levels. The results show that both precipitation intensity and aerosol amount affected the removal effect. A negative removal effect existed for both light precipitation and low $PM_{2.5}$ mass concentration conditions. In contrast, a positive removal effect occurred for both high precipitation and high $PM_{2.5}$ mass concentration conditions. The removal effect increased with increasing precipitation intensity and $PM_{2.5}$ mass concentration before precipitation and was consistent with the change trend of wind speed at a height of 100 m. The findings of this study can help understand the mechanism of wet scavenging on air pollution, providing support for air pollution control in future.

Keywords: precipitation; $PM_{2.5}$; wind; removal effect

1. Introduction

With the rapid development of the economy and urbanization progress in China, more industrial waste gases and particulate matter (PM) have been released to the atmosphere, which threaten the human health and life to a certain extent [1] and have also brought serious ecological and environmental problems [2]. Among various air pollution components, PM with aerodynamic diameters less than 2.5 μm ($PM_{2.5}$) is often the major contributing factor to air pollution [3,4], which has drawn broad attention worldwide.

Aerosol particles can affect the weather and climate by serving as cloud condensation nuclei (CCN) or changing the radiation balance [5–11]. By serving as CCN, aerosol particles can increase cloud droplet number concentration and thus enhance the cloud reflection to solar radiation, which is referred to as the cloud albedo effect [8]. For longwave radiation, by serving as CCN, aerosol particles can increase thin cloud thermal emissivity and trap more longwave radiation within the atmosphere, which is referred to as the cloud thermal emissivity effect [6,11]. These two effects are the shortwave and longwave radiative effects from aerosol-cloud interactions. By reducing cloud droplet effective radius (r_e), aerosol particles could also reduce the efficiency of precipitation and prolong the cloud lifetime, which is referred to as the cloud lifetime effect [5]. In contrast, aerosol can invigorate the convective clouds by releasing more latent heat when freezing, which is referred to as the invigoration effect [12]. These two effects are both the impacts of aerosols on precipitation from the aerosol-cloud interaction. Absorbing aerosol can also burn out the clouds when absorbing solar radiation within clouds, which is referred to as the aerosol semi-direct effect [13].

On the other hand, aerosols can also be affected by weather and climate, such as dispersion by winds and wet scavenging by precipitation. Compared to the studies regarding aerosol effects on weather and climate, the impacts of weather and climate on aerosols are relatively less studied. From the climatological view, aerosols can be influenced by the global warming and large-scale circulation variations, such as the Arctic warming [14], the El Niño event [15], and so on. From the weather view, aerosols can be influenced by various meteorological factors [16]. Solar radiation and water vapor can help the conversion of gases to particles and the growth of fine aerosol particles, and thus increase aerosol concentration [17]. The winds can help disperse and transport aerosol particles to other locations so that the air quality is improved. However, they are still kept within the atmosphere. The mechanism in which the aerosols are really removed from the atmosphere is the dry and wet deposition [18–21]. The dry deposition is the process of direct deposition to the surface by the gravity of the particulate matters or by the absorption of other materials [22,23]. Wet deposition is the process of removing the PM in the air to the surface through precipitation, which plays a significant role in reducing the PM mass concentration in the air [19,24]. The wet deposition process can be divided into intracloud removal and undercloud removal [25]. Undercloud removal, which scavenges fine PM particles under the cloud, is also an important process for the formation of acid rain [26], so it has received widespread attention by the society. Many studies have confirmed the removal effect of precipitation on $PM_{2.5}$ by different methods. For example, Tai et al. [27] established a multivariate linear model to investigate the precipitation scavenging effect on $PM_{2.5}$. Garrett et al. [19] estimated the contribution of precipitation scavenging effect on aerosol amount based on the seasonal variation analysis. Gong et al. [14] applied a generalized additive model to analyze the precipitation scavenging effect on $PM_{2.5}$.

There are various influential factors to the precipitation scavenging effect on $PM_{2.5}$, which have been investigated by recent studies. From the perspective of precipitation, Chate [28] found that the $PM_{2.5}$ mass concentration decreased with the increase of precipitation intensity. Mircea et al. [29] found a linear correlation between the change rate of $PM_{2.5}$ mass concentration and precipitation intensity. Li et al. [30] found that the $PM_{2.5}$ mass concentration and precipitation showed a significant negative correlation. Huang et al. [31] found that the $PM_{2.5}$ mass concentration increased with the increase of precipitation duration, and the correlation was strong. Pranesha et al. [32] found that the change in $PM_{2.5}$ mass concentration is related to the size of raindrops, as raindrops with a diameter greater than 1 mm play a major role in removing $PM_{2.5}$ with a diameter of 1–2 microns. Bae et al. [33] pointed out that the distribution of raindrop size is an important factor for efficiency of undercloud aerosol removal. There are also studies that investigated the precipitation scavenging effect from the perspective of $PM_{2.5}$. Tai et al. [27] found that precipitation removes different types of $PM_{2.5}$ with different efficiencies. Taylor et al. [34] and Andronache et al. [35] found that the removal effect of precipitation on $PM_{2.5}$ is related to the size distribution of $PM_{2.5}$. Sun et al. [21] found that when the $PM_{2.5}$ mass concentration before precipitation is large, the removal effect of precipitation is more obvious.

In recent years, additional meteorological factors (such as winds) have been considered in the analysis about the removal effect of precipitation on $PM_{2.5}$. As known, winds can disperse and transport the aerosol particles to other locations. Gong et al. [14] found that the wind speed is linearly related to the $PM_{2.5}$ mass concentration after logarithm conversion based on a quantitative analysis. Yu et al. [36] indicated that it is easy for winds to blow up the particles attached to the object when the wind speed increases to a certain level, thereby causing the increasing of $PM_{2.5}$ mass concentration [37].

Li et al. [30] found that the wind direction will affect the $PM_{2.5}$ mass concentration by affecting the $PM_{2.5}$ diffusion direction. Chen et al. [16] figured out that the $PM_{2.5}$ mass concentration is affected by various meteorological factors including air pressure, temperature, winds, relative humidity, and so on. However, we should note that most existing studies have taken a single city or site as the research area, which generally has problems in representing a large domain. Moreover, uncertainty remains regarding the impacts of precipitation on $PM_{2.5}$ in China, particularly over the well-known pollution regions.

This study took three typical regions in China as the research areas to investigate the precipitation impacts on concentration of $PM_{2.5}$, and the effects from winds during precipitation period were also briefly discussed. By limiting the particular precipitation events, we intended to identify quantitatively the variation of precipitation impacts on $PM_{2.5}$ with both precipitation intensity and $PM_{2.5}$ amount. The paper is organized as follows. Section 2 provides the study area, data, and method. The analysis and results are presented in Section 3. Section 4 summarizes the findings and gives a discussion.

2. Data and Method

2.1. Region of Interest

This study focused on three typical pollution regions in China, which are the Beijing-Tianjin-Hebei (BTH), the Yangtze River Delta (YRD), and the Pearl River Delta (PRD) regions, as shown in Figure 1. The BTH region lies in Northern China, and belongs to the semihumid area, which is located on the 'leeward slope' on the east side of Taihang Mountains and the south side of Yanshan Mountains, forming a semi-closed terrain. The PRD region, closed to the South China Sea, lies in the southeast of China and has abundant precipitation throughout the year, making the climate warm and humid in this region. Similar to the PRD region, the YRD region also lies in southern China but in northern part of PRD region, generally with less water supply and precipitation.

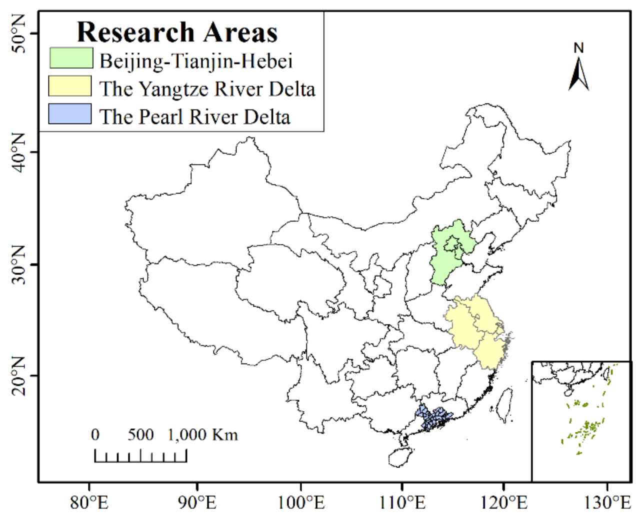

Figure 1. The China map with three typical pollution regions investigated in this study, which are the Beijing-Tianjin-Hebei (BTH), the Yangtze River Delta (YRD), and the Pearl River Delta (PRD) regions.

2.2. Data

Due to the site difference, we selected the observations of precipitation and $PM_{2.5}$ at the same site or closest sites at the same time to form a pair of time series to make further investigation. To avoid the impacts from temporal variation of $PM_{2.5}$ due to either emission or planetary boundary layer variations, we only investigated the hourly precipitation events. For winds near the site, this study analyzed the changes of wind speed over a region around the precipitation site. Note that hourly observation data were adopted in this study.

The precipitation data used in this study was the integration product of ground observation and Climate Prediction Morphing (CMORPH) hourly precipitation products in China. The CMORPH data is a fusion precipitation product with a resolution of 0.1° × 0.1° generated by the National Oceanic and Atmospheric Administration (NOAA) and the Climate Prediction Center (CPC) of the United States Atmospheric and Oceanic Administration. The integration product is generated using a PDF (probability density function matching method) + OI (optimum interpolation method) two-step fusion method based on the observation of precipitation at national automatic sites and the precipitation data retrieved by the CMORPH satellite [38].

The hourly $PM_{2.5}$ mass concentration data used in this study is provided by China National Environmental Monitoring Station, a national air quality real-time publishing platform [39]. $PM_{2.5}$ is measured by the β-ray absorption method and the micro-oscillation balance method, and the reference method is used for testing. The $PM_{2.5}$ data have hourly time resolution and have been qualified officially, and only the data with quality assurance were used in this study.

The hourly reanalysis wind data at 100 m above the ground level from the European Center for Medium-Term Weather Forecast (ECMWF) was used in this study [40]. This data is obtained by applying the laws of physics to combine model data with observational data from all over the world into a global complete and consistent data set, with a spatial resolution of 0.25° × 0.25°. The hourly wind data at the grid that the precipitation site lies in is used to represent the large-scale wind condition at the ground site.

2.3. Method

As indicated earlier, in order to reduce the impact of daily changes in $PM_{2.5}$, this study selected one-hour precipitation events within a relatively stable period (15:00–17:00 Beijing time) of daily $PM_{2.5}$ mass concentration as the research objects. We screened out 1083 cases from 78 sites in the BTH, 5341 cases from 56 sites in the YRD, 2491 cases, from 191 sites in the PRD region for analysis. By doing these data selections, our method was more reliable and meaningful to investigate the precipitation impacts on aerosols, because this processing method limited the natural change of $PM_{2.5}$ due to both planetary boundary layer (PBL) variation or emission variation. Under the premise of clarifying the annual (daily) changes in regional precipitation and $PM_{2.5}$, this study focused on the differences in the removal effect of precipitation on $PM_{2.5}$ under different precipitation intensities and different pollution levels.

According to the studies of Olszowski [41] and Wang and Feng [24], the removal effect (ΔC) of precipitation on $PM_{2.5}$ can be used to represent the change of $PM_{2.5}$ mass concentration after precipitation, which is defined as

$$\Delta C = \frac{C_b - C_p}{C_b} \times 100\%$$

where C_b is the $PM_{2.5}$ mass concentration value before precipitation, and C_p is the $PM_{2.5}$ mass concentration value after precipitation.

When ΔC is larger than 0, the $PM_{2.5}$ mass concentration in the atmosphere decreases with precipitation, which is a positive removal process. In contrast, when it is smaller than 0, the $PM_{2.5}$ mass concentration in the atmosphere increases with precipitation, which is a negative removal process. When it is equal to 0, the mass concentration of $PM_{2.5}$ in the atmosphere has no change, which implies that precipitation plays no role to the $PM_{2.5}$ removal process.

This study focused on the relationship between the removal effect and precipitation intensities, along with the relationship between the removal effect and pollution levels. Based on the number of samples, the precipitation events were divided into three categories according to the precipitation intensity and the $PM_{2.5}$ mass concentration before precipitation to explore their potential differences in the removal effect of the precipitation on the $PM_{2.5}$. In addition, the effect of winds on the $PM_{2.5}$ mass concentration were also investigated and discussed based on hourly winds from ECMWF by selecting typical cases of precipitation events.

3. Analysis and Result

3.1. Temporal Variation of Precipitation and $PM_{2.5}$

Figure 2 shows the monthly variation of precipitation (bar plots) and $PM_{2.5}$ (lines) at three study regions, the BTH, YRD, and PRD regions. For all three study regions, there were clear seasonal variations of precipitation, with maximum values in summer (June, July, and August) and minimum values in winter (December and the following January and February). This should be associated with the Asian monsoon system. In summer, the southeast monsoon prevails and carries abundant water vapor from the Pacific Ocean, which enriches summer precipitation. In contrast, wintertime northwest monsoon from the Eurasian continent causes low water vapor content and high-pressure systems, resulting in much less precipitation.

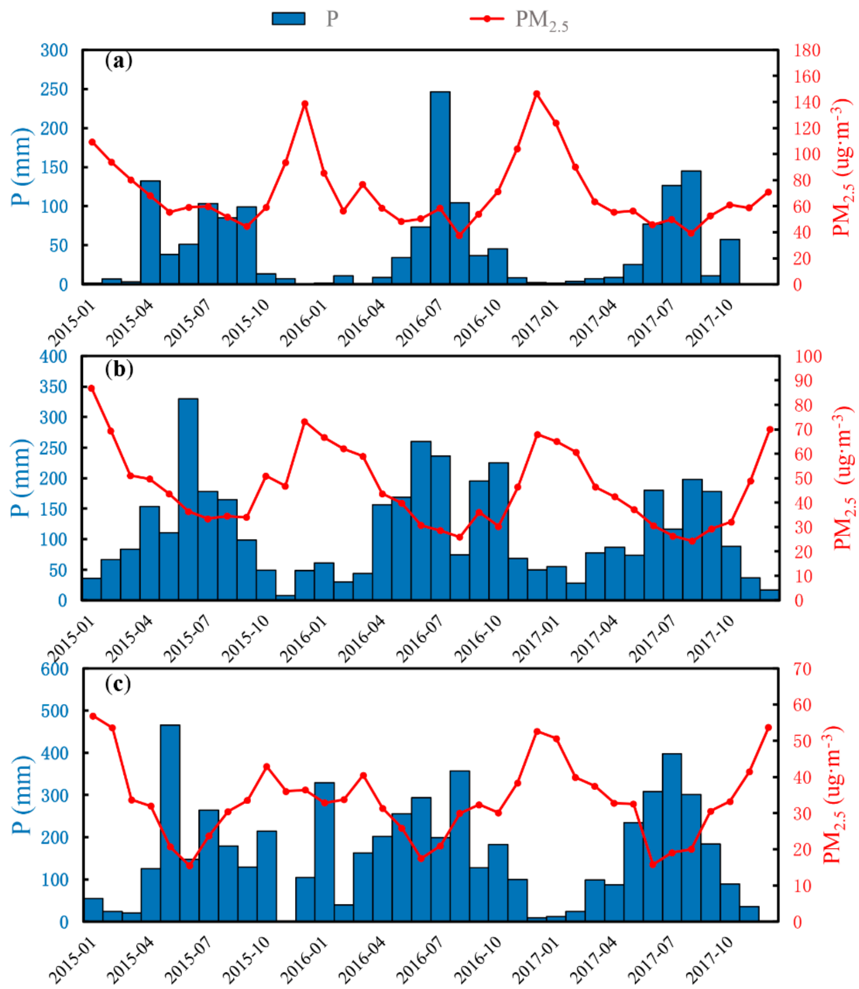

Figure 2. The monthly variations of precipitation and $PM_{2.5}$ mass concentration in the three research areas of (**a**) BTH, (**b**) YRD, and (**c**) PRD.

Statistically, the annual total precipitation amounts in the BTH, YRD, and PRD regions are about 550 mm, 1300 mm, and 1800 mm, respectively. The total annual precipitation in the PRD region is the largest, and in the BTH region is the least. The regional difference is highly related to their relative location in China. As known, the PRD is located in the southeast, closed to the South China Sea, and has sufficient water vapor to provide the necessary support for precipitation. Furthermore, it is located in the subtropical region, with strong solar radiation, which can promote the development of convection and support the formation of precipitation. With lower solar radiation than that in the PRD region, the precipitation in YRD region is slightly less than in the PRD region. It is worth mentioning that due to the frequent occurrence of typhoons in recent years, the YRD and the PRD regions have been seriously affected. Particularly, large amounts of water vapor and then precipitation have been brought to these regions. Differently, the BTH region lies in northern China with insufficient water supply and less precipitation amount.

For the study period, the annual precipitation amount varied with time, with the largest value in 2016 and the lowest value in 2017, and the monthly averaged precipitation amount showed clear temporal variation, with the largest values in July 2016 over BTH region, in June 2015 over the YRD region, and in May 2015 over PRD region. In addition to the Asian monsoon system, the temporal variation of precipitation could be also associated with the El Niño event from 2014 to 2016. For example, due to the influence of El Niño, there was a trend of flooding in the southern China and drought in the northern China in 2015. As a result, April was the month with the highest precipitation in 2015 in BTH region, and the precipitation in June, July, and August significantly decreased compared with the same period in previous years.

Figure 2 also shows the monthly variations of $PM_{2.5}$ mass concentration in BTH, YRD, and PRD regions. Different from precipitation, the monthly variations of $PM_{2.5}$ mass concentration demonstrate the lowest values from June to September and maximum values in December or January. It was found that the $PM_{2.5}$ mass concentration in the BTH region was between 37 to 147 $\mu g \cdot m^{-3}$ in the past three years. According to the $PM_{2.5}$ mass concentration level, there were 25 months with good air quality, 8 months light pollution, and 3 months moderate pollution. The $PM_{2.5}$ mass concentration in the YRD region was between 24 $\mu g \cdot m^{-3}$ to 87 $\mu g \cdot m^{-3}$, which was excellent in air quality for 12 months, good for 22 months, and lightly polluted for 2 months. The $PM_{2.5}$ mass concentration in the PRD region was between 15 $\mu g \cdot m^{-3}$ to 57 $\mu g \cdot m^{-3}$, which was excellent in air quality for 23 months and good for 13 months. Therefore, the air quality in the PRD region was the best in the three years from 2015 to 2017, followed by the YRD, and the worst in BTH region.

The air quality status and temporal variation of $PM_{2.5}$ is the combination resultant of the $PM_{2.5}$ emissions, topography, and meteorological factors. The BTH region is located on the 'leeward slope' on the east side of Taihang Mountains and the south side of Yanshan Mountains, forming a semiclosed terrain. Therefore, the role of the northwest monsoon in autumn and winter seasons is greatly weakened. $PM_{2.5}$ is poorly diffused due to unfavorable meteorological conditions and is easily accumulated. In winter, various human activities, such as coal burning and heating, emit a large amount of $PM_{2.5}$ into the atmosphere and deteriorate the air quality. In contrast, the planetary boundary layer is high and precipitation is strong in summer (as shown in Figure 2), making the $PM_{2.5}$ in BTH region low. Note that the air quality in the BTH area has gradually improved from 2015 to 2017. The $PM_{2.5}$ in the YRD and PRD regions has a poor diffusivity under the influence of long-term 'calm weather' and 'radiation inversion' in winter. Moreover, the relatively high humidity helps the hygroscopic growth of $PM_{2.5}$ particulates, further causing pollution. Similarly, the planetary boundary layer is high and precipitation is strong in summer (as shown in Figure 2), making the $PM_{2.5}$ in YRD and PRD region low. Actually, a good negative relationship between precipitation and $PM_{2.5}$ in seasonal variation has been shown in Figure 2. In next section, we investigate the scavenging effect of precipitation on $PM_{2.5}$.

3.2. *Removal Effect of Precipitation on $PM_{2.5}$*

In order to clearly show the removal effect of precipitation on $PM_{2.5}$, we first examined the diurnal variation of $PM_{2.5}$ mass concentration for cases with and without precipitation over the BTH, YRD, and PRD regions from 2015 to 2017, which is shown in Figure 3. Compared with the averages for cases with precipitation, the averaged mass concentration of $PM_{2.5}$ for cases without precipitation was much larger, along with much more significant diurnal variations. This result implies that significant scavenging effect of precipitation on $PM_{2.5}$ could exist while other influential factors, such as winds and planetary boundary layer, could also play roles. We next investigate the removal effect of precipitation on $PM_{2.5}$ for different precipitation intensities and pollution levels.

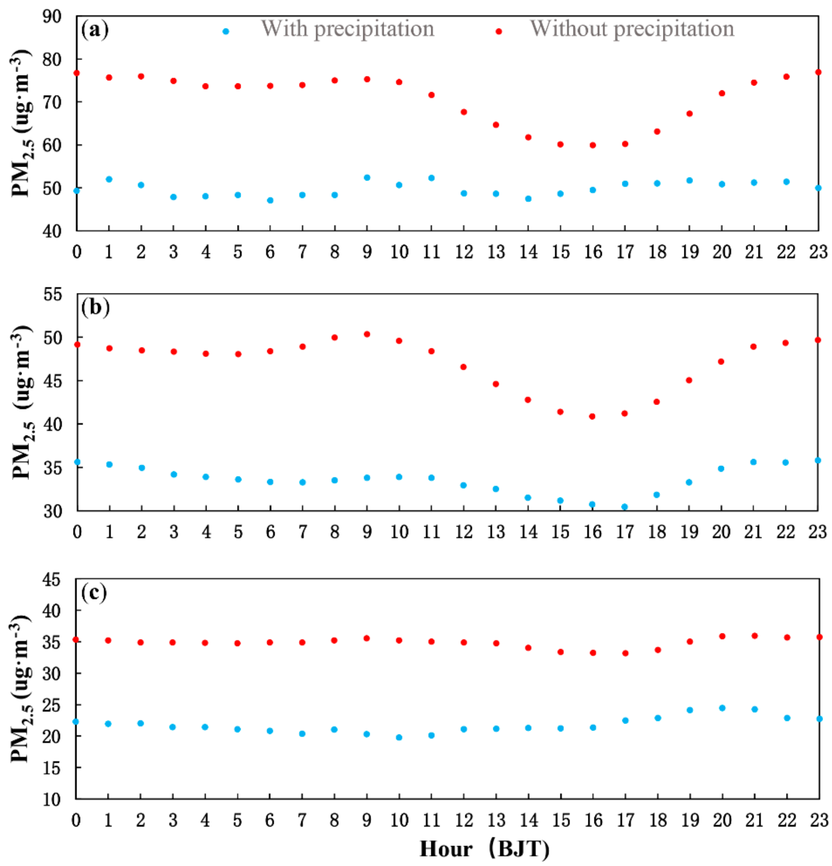

Figure 3. Diurnal variation of $PM_{2.5}$ mass concentration averaged for cases with and without precipitation during the period 2015–2017 over (**a**) BTH, (**b**) YRD, and (**c**) PRD regions. Note the time is Beijing time (BJT).

(a) Removal effect of precipitation on $PM_{2.5}$ under different precipitation intensities

As shown in Figure 3, there are clear diurnal variation of $PM_{2.5}$ mass concentration, mainly due to the diurnal variation of planetary boundary layer (PBL). Several studies have shown that the PBL varies significantly diurnally and seasonally [42–44]. For diurnal variations in the three study regions, it is generally 200–300 m at early morning, increases to about 1000 m around noon and varies little between noon and 17:00 Beijing time, and decreases after 17:00 Beijing time [42]. To isolate the impacts from PBL variation, we investigated the removal effect of precipitation on $PM_{2.5}$ for a period when PBL varies little, which is 15:00–17:00 Beijing time. Considering this time period is short, we only focused on short-term convective precipitation events with duration time no more than one hour. By binning the hourly precipitation with an interval of 0.02 mm/h, Figure 4 shows the variation of precipitation removal effect with precipitation intensity over the BTH, YRD, and PRD regions. Note that three ranges of precipitation intensities have been considered. For all three regions, the removal effects of precipitation on $PM_{2.5}$ had clear variation with precipitation intensity, which changed from negative values to positive values with the increase of precipitation intensity. That is to say, with the increase of precipitation intensity, the removal effect changed from the negative removal process to the positive removal process. This finding is consistent with that found by Sun et al. [21] When the precipitation intensity is low, the negative value of removal effects indicates that $PM_{2.5}$ mass concentration increases while the increased amount is generally less than 20%. A likely explanation is as follows. When the precipitation is weak, the scavenging effect due to the collision of precipitation droplets and $PM_{2.5}$ particles is generally low, but the hygroscopic growth of aerosol particles associated with the high humidity becomes strong, which results in an increasing combination effect on $PM_{2.5}$ mass concentration. With the increase of precipitation intensity, the collision efficiency becomes larger and so as the precipitation scavenging effects, which will result in a more positive removal effect of precipitation on $PM_{2.5}$. At the same time, heavy precipitation is often accompanied by strong winds, which further improves the $PM_{2.5}$ diffusion capacity, reducing more the $PM_{2.5}$ mass concentration.

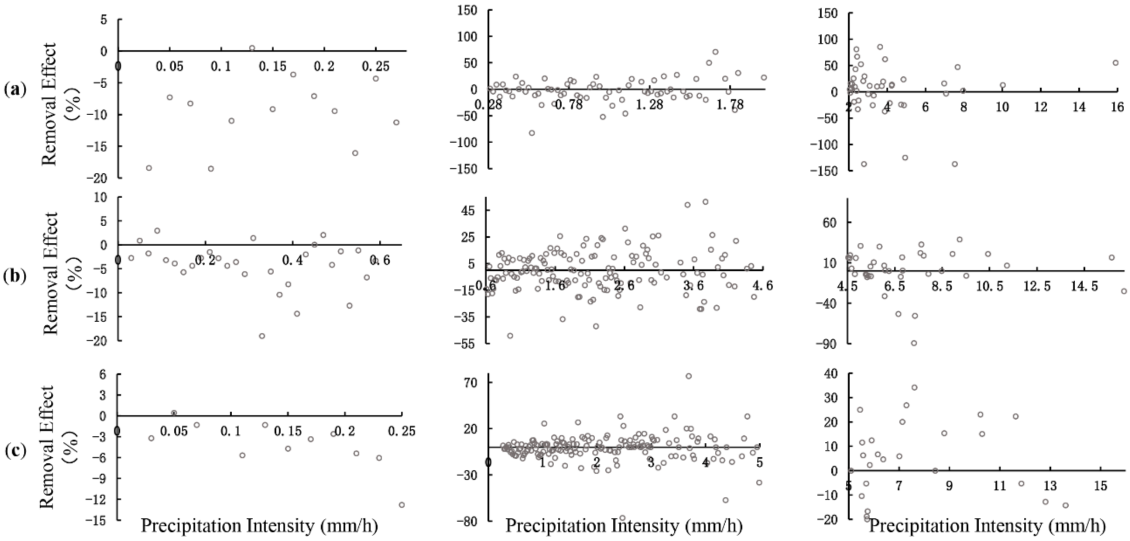

Figure 4. Scatterplot of removal effect versus precipitation intensity for three different ranges of precipitation intensities over (**a**) BTH, (**b**) YRD, and (**c**) PRD regions. Note that the three different ranges of precipitation intensities are classified for negative, neutral, and positive dominant precipitation removal effects, respectively.

The removal effects over the three areas all showed the same change law with precipitation intensity, but there were also differences. In BTH region, the negative removal process was dominant when the precipitation intensity was less than 0.28 mm/h, and the positive removal process was dominant when the precipitation intensity was more than 2 mm/h. For precipitation intensity between 0.28 and 2 mm/h, the removal efficiency slightly increased with intensity (from negative to positive) in tendency, but values fluctuated around the 0 value. In other words, there were three stages of removal effects (negative, roughly neutral, and positive) with precipitation intensities. The removal effect also showed the same three stages in the YRD and PRD regions, but with different threshold values of precipitation intensities. The three stages were for precipitation intensities less than 0.6 mm/h, 0.6 to 4.5 mm/h, and more than 4.5 mm/h in the YRD region, and for precipitation intensities less than 0.25 mm/h, 0.25 to 5 mm/h, and more than 5 mm/h in the PRD region.

Shortly, for precipitation intensities less than 0.28 mm/h, 0.6 mm/h, and 0.25 mm/h, the $PM_{2.5}$ mass concentration increased with precipitation amount in the BTH, YRD and PRD regions, respectively. The threshold values for the negative removal effects were small and close to each other in values among the three regions. In contrast, for precipitation intensities larger than 2 mm/h, 4.5 mm/h, and 5 mm/h, the $PM_{2.5}$ mass concentration decreased with precipitation amount in the BTH, YRD, and PRD regions, respectively. This result is similar to the findings of Kluska et al. [45]. They took Rzeszów (SE Poland) as the research area and found that aerosol concentrations (pollen) decreased only for precipitation intensities less than approximately 5 mm/h, which indicates that precipitation only decreases the aerosol concentration when the precipitation intensity is greater than a certain value. Combined with the findings from Kluska et al. [45], the critical value of precipitation intensity below which the aerosol concentration increases with precipitation is different among different regions. Since the removal efficiency is dependent on both the hygroscopic growth of aerosols and the collision-coalescence efficiency of precipitation droplets, the threshold values of precipitation intensity for both negative and positive removal efficiencies should be related to both $PM_{2.5}$ and precipitation properties, along with the potential impacts from other meteorological components such as winds. In next section, the change of removal efficiency to $PM_{2.5}$ mass concentration is further investigated.

To confirm the findings in this section, we conducted further analysis by dividing the precipitation into three groups with equal sample size according to the precipitation intensity. Correspondingly, the threshold values of precipitation intensities for the classifications were 0.16 mm/h and 0.40 mm/h over BTH region, 0.16 mm/h and 0.36 mm/h over YRD region, and 0.20 mm/h and 0.56 mm/h over PRD region. With this classification, both positive and negative removal effects were found at different precipitation intensity ranges. We then counted the percentages of samples with positive or negative removal effects, which are shown in Table 1 for BTH, YRD, and PRD regions. As can be seen from Table 1, when the precipitation intensity increased, the sample percentage with positive removal effect gradually increased, and the sample percentage with negative removal effect gradually decreased. However, the decreasing (increasing) trend of positive (negative) removal effect with precipitation amount was as clear as that shown in Figure 4. A potential reason is that the threshold values for equal sample size analysis were too close to each other due to the large amount of weak precipitation, which made the differences among the three ranges small. Actually, there were even abnormal trends in the YRD (the sample percentage with positive removal efficiency increased first and then decreased with the intensity of precipitation) and PRD regions (the sample percentage with negative removal efficiency decreased first and then increased with precipitation intensity). More potential reasons are further discussed with case analysis in next section.

Table 1. Sample percentage with positive, neutral, and negative removal effect for three equal-sample bins of precipitation intensity in the BTH, YRD, and PRD regions.

	BTH			**YRD**			**PRD**		
Precipitation (mm/h)	<0.16	[0.16,0.40)	≥0.40	≤0.16	(0.16,0.36]	>0.36	<0.20	[0.20,0.56)	≥0.56
Sample percentage with positive removal effect (%)	41.28	45.31	49.58	43.86	44.76	44.17	36.33	37.59	42.79
Sample percentage with neutral removal effect (%)	6.10	4.43	7.32	10.44	10.93	11.23	17.16	15.85	16.11
Sample percentage with negative removal effect (%)	52.62	50.26	43.10	45.70	44.31	44.60	46.51	46.56	41.10

(b) Removal effect of precipitation on $PM_{2.5}$ under different pollution levels

We classified the $PM_{2.5}$ into three groups with the same sample volume based on $PM_{2.5}$ mass concentration before precipitation, and then further analyzed the change of precipitation removal effect on $PM_{2.5}$. The threshold values of $PM_{2.5}$ for the three-group classification were 25 $\mu g \cdot m^{-3}$ and 55 $\mu g \cdot m^{-3}$ over TBH, 19 $\mu g \cdot m^{-3}$ and 37 $\mu g \cdot m^{-3}$ over YRD, and 14 $\mu g \cdot m^{-3}$ and 26 $\mu g \cdot m^{-3}$ over PRD.

Table 2 shows the sample frequencies with positive, negative, and neutral removal effects over the three study regions. For all three study regions, it is clear that the negative removal effect of precipitation dominated at low $PM_{2.5}$ mass concentration condition, and the sample frequency with negative removal effect of precipitation decreased with $PM_{2.5}$ mass concentration. In contrast, the sample frequency with positive removal effect of precipitation increased with $PM_{2.5}$ mass concentration, and the positive removal effect played a dominant role under heavy pollution condition. A likely explanation is that the collision-coalescence effect increased with $PM_{2.5}$ mass concentration due to the increased particle density, which made the precipitation scavenging effect more prominent at heavy pollution condition. Differently, when the $PM_{2.5}$ mass concentration was low, the collision-coalescence effect was weak, and the hygroscopic growth of aerosol particles could be prominent instead, making the negative removal cases more frequent.

Table 2. Sample percentage with positive, neutral, and negative removal effect for three equal-sample bins of pollution levels in the BTH, YRD, and PRD regions.

	BTH			**YRD**			**PRD**		
Pollution (μg/m^3)	≤25	(25,55]	>55	≤19	(19,37]	>37	≤14	(14,26]	>26
Sample percentage with positive removal effect (%)	32.87	49.44	53.99	33.41	45.38	54.17	25.42	40.91	50.94
Sample percentage with neutral removal effect (%)	8.01	6.70	3.03	17.18	9.63	5.74	25.54	15.27	7.93
Sample percentage with negative removal effect (%)	59.12	43.86	42.98	49.41	44.99	40.09	49.04	43.82	41.13

Considering that the removal effect of precipitation on $PM_{2.5}$ depends on both precipitation intensity and $PM_{2.5}$ amount, Figure 5 shows the change of removal effect of precipitation for three equal-sample bins of precipitation intensities under three different $PM_{2.5}$ mass concentration conditions over the BTH, YRD, and PRD regions. Consistent with the findings from Tables 1 and 2 for similar precipitation intensity, the removal effect increased with the increase of $PM_{2.5}$ mass concentration, that is, the precipitation scavenging was more effective when $PM_{2.5}$ mass concentration before precipitation was higher. For a similar $PM_{2.5}$ mass concentration before precipitation, the removal effect roughly increased with the increase of precipitation intensity. Note that the negative removal effect values under low $PM_{2.5}$ mass concentration conditions were clearly larger than the positive removal effect values under high $PM_{2.5}$ mass concentration conditions. A likely reason is that the $PM_{2.5}$ mass concentration before precipitation was much smaller at low $PM_{2.5}$ mass concentration conditions, making the removal efficiency (relative change of $PM_{2.5}$ mass concentration) much higher than that for heavy pollution conditions.

(c) Case analysis

Figure 5 shows that under low $PM_{2.5}$ mass concentration conditions, the negative removal effect decreased first and then increased with precipitation intensity over BTH, and increased first and then decreased with precipitation intensity over YRD. Under moderate $PM_{2.5}$ mass concentration conditions, the removal effect increased first and then decreased with precipitation intensity over PRD. These results imply that other influential factor than precipitation, such as winds, could also affect the $PM_{2.5}$ mass concentration simultaneously. We here give a brief discussion about the winds impact on the precipitation removal effect to $PM_{2.5}$ using case analysis.

The average wind speed, at a height of 100 m within a domain of 0.25° × 0.25° where the study site is located, was explored for three selected cases in the three study regions. The three selected precipitation event cases are those which occurred at the site of Tangshan Ceramic Company (118.22° E, 39.67° N) in the BTH region at 17:00 on 12 March 2016, at the site of the Zhenjiang Vocational Education Center (119.49° E, 32.22° N) in the YRD region at 16:00 on 26 June 2016, and at the Nanyou Station in Shenzhen City (113.92° E, 22.52° N) in the PRD region at 16:00 on 5 September 2017. Note that for these three cases, the precipitation intensity and $PM_{2.5}$ mass concentrations were all different. For the BTH region case, the precipitation intensity was 3.25 mm/h and the $PM_{2.5}$ mass concentration before precipitation was 90 μg/m^3. For the YRD region case, the precipitation intensity was 6.76 mm/h and the $PM_{2.5}$ mass concentration before precipitation was 51 μg/m^3. For the PRD region case, the precipitation intensity was 5.70 mm/h and the $PM_{2.5}$ mass concentration before precipitation was 18 μg/m^3.

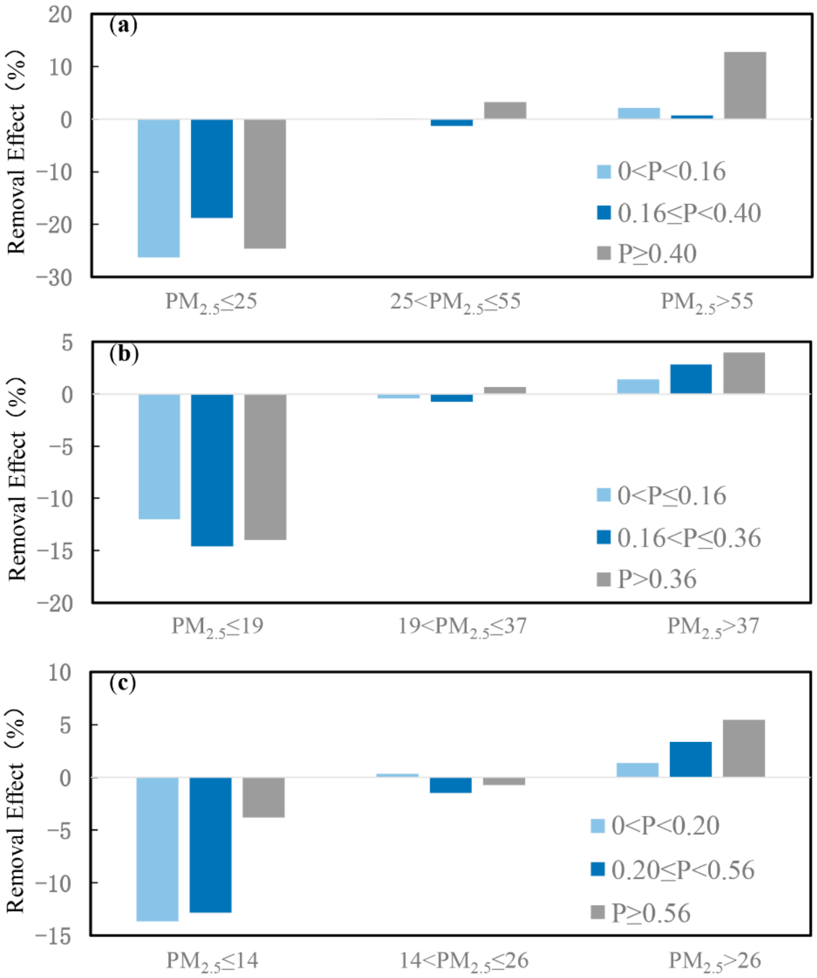

Figure 5. Differences in removal effect of precipitation under different precipitation intensity (unit mm/hour) and $PM_{2.5}$ mass concentration (before precipitation) (unit μg/m^3) conditions over (**a**), BTH, (**b**) YRD, and (**c**) PRD regions.

Figure 6 shows the hourly variation of wind speed (at a height of 100 m above surface) and removal effect of precipitation on $PM_{2.5}$ from 15:00 to 23:00 on the study day over the BTH, YRD, and PRD regions. Note that the precipitation event was still an event with a duration time of no more than one hour, while the $PM_{2.5}$ mass concentration at different hours after precipitation was used for the calculation of removal effect at that time in Figure 6. Roughly, the precipitation removal effect and the wind speed had a similar hourly variation trend. This could be easily understood since the winds can enhance the diffusivity of $PM_{2.5}$ and reduce its mass concentration. Figure 6 shows that the wind speeds at the hour when precipitation event occurred in BTH (17:00), YRD (16:00) and PRD (16:00) regions were about 4 m/s, 2 m/s, and 3 m/s, and the removal efficiencies at those hours were all negative. This suggests that even with considerable wind speeds, the $PM_{2.5}$ still likely increases with precipitation for particular cases due to the aerosol's hygroscopic growth. However, when the winds are large enough, such as more than 4.7 m/s, 3.1 m/s, and 6.6 m/s over BTH, YRD and PRD, the impacts of winds could cause the removal effect change from negative values to positive values. Of course, when the precipitation is large, the positive removal effect of precipitation on $PM_{2.5}$ could be further enhanced by the accompanied winds. Gong et al. [14] also found the significant removing effects of winds on $PM_{2.5}$ particles, which indicated that nearly 60% of $PM_{2.5}$ mass concentrations could be reduced when the wind speed was up to 6 m/s. Thus, the combination of precipitation and winds could enhance the removal effects of precipitation on $PM_{2.5}$, which is definitely worthy of further investigation in future.

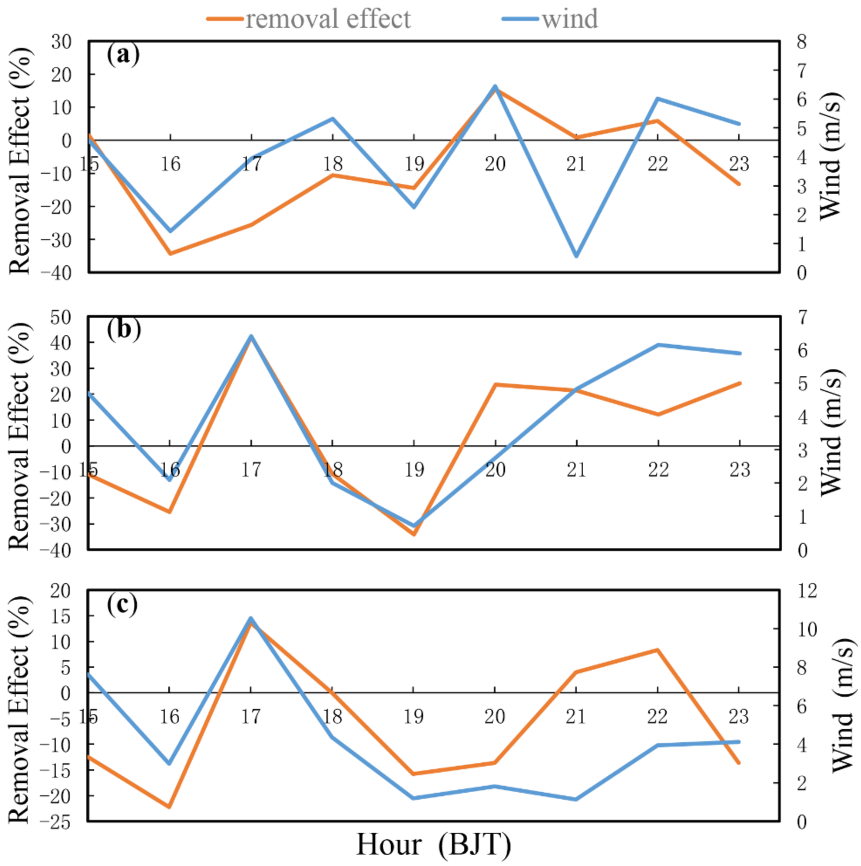

Figure 6. Hourly variation of removal effect of precipitation and wind speed at a height of 100 m above the ground for selected precipitation event cases at the site of Tangshan Ceramic Company (118.22° E, 39.67° N) in the BTH region at 17:00 on 12 March 2016 (**a**), at the site of the Zhenjiang Vocational Education Center (119.49° E, 32.22° N) in the YRD region at 16:00 on 26 June 2016 (**b**), and at the Nanyou Station in Shenzhen City (113.92° E, 22.52° N) in the PRD region at 16:00 on 5 September 2017 (**c**). "BJT" represents Beijing time.

4. Conclusions

Seasonal variations of precipitation and $PM_{2.5}$ mass concentration were investigated first. The precipitation intensity showed clear seasonal variation, with maximum values in summer and minimum values in winter for all three study regions of the Beijing-Tianjin-Hebei (BTH), the Yangtze River Delta (YRD), and the Pearl River Delta (PRD) regions. This is highly associated with the Asian monsoon system, including both the southeast and southwest summer Monsoon and northwest winter monsoon. Due to these monsoon system and water supply, the precipitation amount was the largest in the PRD region and the smallest in BTH region. Abnormal changes in the seasonal variations were also affected by the El Niño events. Similar seasonal variations have been found for $PM_{2.5}$ mass concentration, implying the potential removal effects of precipitation on $PM_{2.5}$, while other meteorological components, such as winds and planetary boundary layer heights, can also affect the $PM_{2.5}$ mass concentration. In all three study regions, the $PM_{2.5}$ mass concentration under clear sky was much larger than that under precipitation conditions, also implying the potential removal effect of precipitation on $PM_{2.5}$.

The removal effect of precipitation on $PM_{2.5}$ was then investigated. The study shows that the removal effect of precipitation on $PM_{2.5}$ is dependent on both the precipitation intensity and $PM_{2.5}$ mass concentration, along with other coexisting meteorological components. We found that the negative removal effect dominated when the intensity of precipitation was weak. With the increase of precipitation intensity, the removal effect of precipitation on $PM_{2.5}$ changed from negative to positive values gradually. When the precipitation was heavy, the positive removal effect dominated and reduced the $PM_{2.5}$ mass concentration clearly. A likely mechanism has been proposed: The hygroscopic growth of aerosols plays a more (less) important effect than the collision-coalescence between precipitation droplets and aerosols when the precipitation is weak (strong), making $PM_{2.5}$ mass concentration increase (decrease). Further analysis using the equal-sample bins of precipitation data confirmed these results. By binning the $PM_{2.5}$ mass concentration into three groups with the same sample size, this study found that the negative removal effect dominated for low $PM_{2.5}$ mass concentration condition, and positive removal effect dominated for high $PM_{2.5}$ mass concentration condition. This was likely due to the increasing collision-coalescence efficiency of precipitation with aerosol particles when aerosol density (so $PM_{2.5}$) increased. Shortly, the removal effect was higher when the pollution was heavier and precipitation was stronger.

The impacts of wind speed on the removal effect of precipitation were finally discussed using case studies based on wind speed at 100 m above the surface. As expected, a positive relationship was found between removal effect and wind speed. However, negative removal effects were still found for three cases when the wind speed was high, which indicates that the hygroscopic growth effect was prominent for particular cases. We can also expect that the positive removal effect by precipitation when precipitation or pollution is heavy could be enhanced by the accompanied winds.

Author Contributions: Methodology, X.Z.; Investigation, H.J.; writing—original draft preparation, X.Z.; writing—review and editing, C.Z., Y.S. All authors have read and agree to the published version of the manuscript.

Funding: This work was funded by the National Natural Science Foundation of China (NSFC) (41925022), the Ministry of Science and Technology of China National Key R&D Program (2019YFA0606803, 2017YFC1501403), the Hebei Province Key Research and Development project (20375402D), the Beijing Municipal Commission of science and technology (grant D171100007917001), and the State Key Laboratory of Earth Surface Processes and Resource Ecology.

Acknowledgments: Data used in this study are available online from http://cdc.cma.gov.cn/sksj.do?method=ssrjscprh, http://beijingair.sinaapp.com and https://www.ecmwf.int/en/forecasts/datasets/reanalysis-datasets/era5.

Conflicts of Interest: The authors declare no conflict of interest.

References

1. Lelieveld, J.; Evans, J.S.; Fnais, M.; Giannadaki, D.; Pozzer, A. The contribution of outdoor air pollution sources to premature mortality on a global scale. *Nature* **2015**, *525*, 367–371. [CrossRef] [PubMed]
2. Guan, D.; Su, X.; Zhang, Q.; Peters, G.P.; Liu, Z.; Lei, Y.; He, K. The socioeconomic drivers of China's primary $PM_{2.5}$ emissions. *Environ. Res. Lett.* **2014**, *9*, 024010. [CrossRef]
3. Fan, H.; Zhao, C.; Yang, Y. A comprehensive analysis about the spatio-temporal variation of urban air pollution in China during recent years of 2014–2018. *Atmos. Environ.* **2020**, *220*, 117066. [CrossRef]
4. Pui, D.Y.H.; Chen, S.; Zuo, Z. $PM_{2.5}$ in China: Measurements, sources, visibility and health effects, and mitigation. *Particuology* **2014**, *13*, 1–26. [CrossRef]
5. Albrecht, B. Aerosol, cloud microphysics, and fractional cloudiness. *Science* **1989**, *245*, 1227–1230. [CrossRef] [PubMed]
6. Garrett, T.J.; Zhao, C. Increased Arctic cloud longwave emissivity associated with pollution from mid-latitudes. *Nat. Int. Wkly J. Sci.* **2006**, *440*, 787–789. [CrossRef]
7. Jahani, B.; Calbó, J.; González, J.A. Transition zone radiative effects in shortwave radiation parameterizations: Case of weather research and forecasting model. *J. Geophys. Res. Atmos.* **2019**, *124*, 13091–13104. [CrossRef]
8. Twomey, S. Influence of Pollution on Shortwave Albedo of Clouds. *J. Atmos. Sci.* **1977**, *34*, 1149–1152. [CrossRef]
9. Verma, S.; Venkataraman, C.; Bouche, O. Attribution of aerosol radiative forcing over India during the winter monsoon to emissions from source categories and geographical regions. *Atmos. Environ.* **2011**, *45*, 4398–4407. [CrossRef]
10. Zhao, C.; Lin, Y.; Wu, F.; Wang, Y.; Li, Z.; Rosenfeld, D.; Wang, Y. Enlarging rainfall area of tropical cyclones by atmospheric aerosols. *Geophys. Res. Lett.* **2018**, *45*, 8604–8611. [CrossRef]

11. Zhao, C.; Garrett, T.J. Effects of Arctic haze on surface cloud radiative forcing. *Geophys. Res. Lett.* **2015**, *42*, 557–564. [CrossRef]
12. Rosenfeld, D.; Lohmann, U.; Raga, G.B.; O'Dowd, C.D.; Kulmala, M.; Fuzzi, S.; Reissell, A.; Andreae, M.O. Flood or drought: How do aerosols affect precipitation? *Science* **2008**, *321*, 1309–1313. [CrossRef] [PubMed]
13. Ramaswamy, V.; Boucher, O.; Haigh, J.; Hauglustaine, D.; Haywood, J.; Myhre, G.; Nakajima, T.; Shi, G.Y.; Solomon, S. *Radiative forcing of climate change. Climate Change 2001: The Scientic Basis. Contribution of Working Group I to the Third Assessment Report of the Intergovernmental Panel on Climate Change*; Houghton, J.T., Dingis, Y., Griggsis, D.J., Nogueris, M., van der Lindenis, P.J., Daiis, X., Maskellis, K., Johnsonis, C.A., Eds.; Cambridge University Press: Cambridge, UK, 2001; pp. 349–416.
14. Gong, C.; Zhang, B.; Tang, X.; Xu, G.; Zhou, Y.; Zhou, L.; Zhao, S. Influences of wind and precipitation on different-sized particulate matter concentrations ($PM_{2.5}$, PM_{10}, $PM_{2.5\text{-}10}$). *Meteorol. Atmos. Phys.* **2018**, *130*, 383–392.
15. Ruchith, R.D.; Sivakumar, V. Influence of aerosol-cloud interaction on austral summer precipitation over Southern Africa during ENSO events. *Atmos. Res.* **2018**, *202*, 1–9. [CrossRef]
16. Chen, Z.; Chen, D.; Zhao, C.; Kwan, M.P.; Cai, J.; Zhuang, Y.; Zhao, B.; Wang, X.; Chen, B.; Yang, J.; et al. Influence of meteorological conditions on $PM_{2.5}$ concentrations across China: A review of methodology and mechanism. *Environ. Int.* **2020**, *139*, UNSP105558. [CrossRef] [PubMed]
17. Zhao, C.; Li, Y.N.; Zhang, F.; Sun, Y.L.; Wang, P.C. Growth rates of fine aerosol particles at a site near Beijing in June 2013. *Adv. Atmos. Sci.* **2018**, *35*, 209–217. [CrossRef]
18. Atlas, E.; Giam, C.S. Ambient concentration and precipitation scavenging of atmospheric organic pollutants. *Water Air Soil Pollut.* **1988**, *38*, 19–36.
19. Garrett, T.J.; Zhao, C.; Novelli, P.C. Assessing the relative contributions of transport efficiency and scavenging to seasonal variability in Arctic aerosol. *Tellus B* **2010**, *62*, 190–196. [CrossRef]
20. Radke, L.F.; Hobbs, P.V.; Eltgroth, M.W. Scavenging of Aerosol Particles by Precipitation. *J. Appl. Meteorol. (1962–1982)* **1980**, *19*, 715–722.
21. Sun, Y.; Zhao, C.; Su, Y.; Ma, Z.; Li, J.; Husi, L.; Yang, Y.; Fan, H. Distinct impacts of light and heavy precipitation on $PM_{2.5}$ mass concentration in Beijing. *Earth Space Sci.* **2019**, *6*, 1915–1925. [CrossRef]
22. Wesely, M.L.; Hicks, B.B. A review of the current status of knowledge on dry deposition. *Atmos. Environ.* **2000**, *34*, 2261–2282. [CrossRef]
23. Zhang, L.; Gong, S.; Padro, J.; Barrie, L. A size-segregated particle dry deposition scheme for an atmospheric aerosol module. *Atmos. Environ.* **2001**, *35*, 549–560. [CrossRef]
24. Wang, S.; Feng, X. Influence of different weather events on concentrations of particulate matter with different sizes in Lanzhou, China. *J. Environ. Sci.* **2012**, *24*, 665–674. [CrossRef]
25. Steinfeld, J.H.; Pandis, S.N. Atmospheric chemistry and physics: From air pollution to climate change. *Environ. Sci. Policy Sustain. Dev.* **1998**, *40*, 1203. [CrossRef]
26. Luan, T.; Guo, X.; Zhang, T.; Guo, L. Below-cloud aerosol scavenging by different intensity rains in Beijing city. *J. Meteorol. Res.* **2019**, *33*, 126–137. [CrossRef]
27. Tai, A.P.K.; Mickley, L.J.; Jacob, D.J. Correlations between fine particulate matter ($PM_{2.5}$) and meteorological variables in the United States: Implications for the sensitivity of $PM_{2.5}$ to climate change. *Atmos. Environ.* **2010**, *44*, 3976–3984. [CrossRef]
28. Chate, D.M. Study of scavenging of submicron-sized aerosol particles by thunderstorm rain events. *Atmos. Environ.* **2005**, *39*, 6608–6619. [CrossRef]
29. Mircea, M.; Fuzzi, S.; Stefan, S. Precipitation scavenging coefficient: Influence of measured aerosol and raindrop size distributions. *Atmos. Environ.* **2000**, *34*, 5169–5174. [CrossRef]
30. Li, X.; Li, X.; Feng, Y.; Liang, H. The impact of meteorological factors on $PM_{2.5}$ variations in Hong Kong. *IOP Conf. Ser. Earth Environ. Sci.* **2017**, *78*, 12003–12010. [CrossRef]
31. Huang, Y.; Wu, S.; Chen, X. Temporal distribution characteristics of $PM_{2.5}$ and meteorological conditions in Anqing in recent four years. *Meteorol. Environ. Res.* **2020**, *11*, 7–9.
32. Pranesha, T.S.; Kamra, A.K. Scavenging of aerosol particles by large water drops: 3. Washout coefficients, half-lives, and rainfall depths. *J. Geophys. Res. Atmos.* **1997**, *102*, 23947–23953. [CrossRef]
33. Bae, S.Y.; Woo, J.; Park, R.J.; Kim, Y.P. Effects of below-cloud scavenging on the regional aerosol budget in East Asia. *Atmos. Environ.* **2012**, *58*, 14–22.

34. Taylor, P.A.; Michelangeli, D.V.; Zhang, L. Numerical studies of aerosol scavenging by low-level, warm stratiform clouds and precipitation. *Atmos. Environ.* **2004**, *38*, 4653–4665.
35. Andronache, C. Estimated variability of below-cloud aerosol removal by rainfall for observed aerosol size distributions. *Atmos. Chem. Phys.* **2003**, *3*, 131–143.
36. Yu, C.; Deng, X.; Shi, C.; Wu, B.; Zhai, J.; Yang, G.; Huo, Y. Analysis of the removal effect of precipitation and wind on atmospheric $PM_{2.5}$ and PM_{10}. *Acta Sci. Circumst.* **2018**, *38*, 4620–4629. (In Chinese)
37. Rahmati, O.; Mohammadi, F.; Ghiasi, S.S.; Tiefenbacher, J.; Moghaddam, D.D.; Coulon, F.; Nalivan, O.A.; Bui, D.T. Identifying sources of dust aerosol using a new framework based on remote sensing and modelling. *Sci. Total Environ.* **2020**, *737*, 139508. [CrossRef]
38. Precititation from Chinese Meteorology Administration. Available online: http://cdc.cma.gov.cn/sksj.do?method=ssrjscprh (accessed on 1 March 2020).
39. PM2.5 from Beijing Air Quality Platform. Available online: http://beijingair.sinaapp.com (accessed on 1 March 2020).
40. Winds from ECMWF. Available online: https://www.ecmwf.int/en/forecasts/datasets/reanalysis-datasets/era5 (accessed on 27 April 2020).
41. Olszowski, T. Changes in PM_{10} concentration due to large-scale rainfall. *Arab. J. Geosci.* **2016**, *9*, 160. [CrossRef]
42. Guo, J.; Miao, Y.; Zhang, Y.; Liu, H.; Li, Z.; Zhang, W.; He, J.; Lou, M.; Yan, Y.; Bian, L. The climatology of planetary boundary layer height in China derived from radiosonde and reanalysis data. *Atmos. Chem. Phys.* **2016**, *16*, 13309–13319. [CrossRef]
43. Liu, S.; Liang, X. Observed diurnal cycle climatology of planetary boundary layer height. *J. Clim.* **2010**, *23*, 5790–5809. [CrossRef]
44. Liu, N.; Zhou, S.; Liu, C.; Guo, J. Synoptic circulation pattern and boundary layer structure associated with $PM_{2.5}$ during wintertime haze pollution episodes in Shanghai. *Atmos. Res.* **2019**, *228*, 186–195. [CrossRef]
45. Kluska, K.; Piotrowicz, K.; Kasprzyk, I. The impact of rainfall on the diurnal patterns of atmospheric pollen concentrations. *Agric. For. Meteorol.* **2020**, *291*, 108042. [CrossRef]